

PACS numbers: 42.55.Px; 42.81.Wg; 42.60.Da; 42.79.Jq
DOI: 10.1070/QE2006v036n04ABEH013144

Tunable semiconductor laser with an acousto-optic filter in an external fibre cavity

E.V. Andreeva, L.N. Magdich, D.S. Mamedov,
A.A. Ruenkov, M.V. Shramenko, S.D. Yakubovich

***Abstract*. A tunable semiconductor laser with a laser amplifier based on a double-pass superluminescent diode as an active element and an acousto-optic filter in an external fibre cavity as a selective element is investigated. A continuous spectral tuning is achieved in a band of width 60 nm centered at a wavelength of 845 nm and the 'instant' linewidth below 0.05 nm is obtained. The sweep frequency within the tuning range achieves 200 Hz. The cw power at the output of a single-mode fibre was automatically maintained constant at the level up to 1.5 mW.**

Keywords: *tunable laser, semiconductor optical amplifier, superluminescent diode, acousto-optic tunable filter, optical coherence tomography*.

1. Introduction

Tunable semiconductor lasers have been studied in a vast number of publications. Dozens of models of these devices are now available in the optoelectronic market. These lasers use most often optical schemes with an external cavity containing a tunable spectrally selective element. In this paper, we solved the problem of the development of a prototype of a specialised near-IR source for new systems of optical coherence tomography. The main technical requirements imposed upon this source are a sufficiently broad tuning range (more than 50 nm), the possibility of a relatively fast (at a frequency of higher than 100 Hz) sweep of the radiation wavelength and coupling radiation out through a single-mode fibre (SMF). The requirement to the 'instant' spectral linewidth $\delta\lambda$ is quite modest ($\delta\lambda < 0.1$ nm).

With these requirements in mind, we decided to use a semiconductor optical amplifier (SOA) based on double-pass superluminescent diodes (SLDs) made of a single-layer quantum-well structure (SQW) [1, 2] as an active element and as a spectrally selective element in an external fibre cavity – an acousto-optic tunable filter (AOTF). The advantages of these filters, which are rarely used in tunable semiconductor lasers [3, 4], are a broad tuning range and a sufficiently fast response, while their disadvantages are a relatively large size, a rather strong temperature dependence of operating characteristics, and a high energy consumption. In our case, these drawbacks did not prevent the use of an AOTF because this device was applied in laboratory experiments.

E.V. Andreeva, D.S. Mamedov, A.A. Ruenkov, M.V. Shramenko Superlum Diodes Limited Liability Company, P.O. Box 70, 117454 Moscow, Russia; e-mail: andreeva@superlumdiodes.com, mamedov@superlumdiodes.com, shramenko@superlumdiodes.com;
L.N. Magdich M.F. Stel'makh Polyus Research & Development Institute, ul. Vvedenskogo 3, 117342 Moscow, Russia; e-mail: lmagdich@mtu-net.ru;
S.D. Yakubovich Moscow State Institute of Radio Engineering, Electronics and Automatics (Technical University), prosp. Vernadskogo 78, 119454 Moscow, Russia; e-mail: yakubovich@superlumdiodes.com

Received 1 December 2005
Kvantovaya Elektronika **36** (4) 324 – 328 (2006)
Translated by M.N. Sapozhnikov

2. Laser components and design

A double-pass SLD was fabricated using the known design with a bent active channel [5]. The end of the bent part of the active waveguide, whose axis made an angle 7° with the normal to the output facet of the crystal, was covered with an antireflection dielectric coating. To optimise this element, it was necessary to determine the length of the active channel, the reflection coefficient of the rear end facet oriented normally to the active-channel axis, and the operating injection current providing a sufficiently high level of the double-pass optical gain for the maximum width of the gain spectrum and rather small residual modulation by the Fabry – Perot modes. We determined the design and operating regime of the SLD providing the values of the latter three parameters equal to 20 dB, 45 nm, and 3 %, respectively. The SOA modules were assembled in standard Butterfly housings with coupling out radiation through a polarisation-maintaining PANDA SMF. The 'slow' axis of the fibre corresponded to the TE polarisation of radiation.

Figure 1 presents the typical light – current characteristics and emission spectra of these modules. In the SLD regime in the absence of a positive optical feedback, the output characteristics are similar to those of conventional SLDs based on the given SQW. When a cleave with the reflection coefficient 4 % was made perpendicular to the output SMF axis, these characteristics acquired a distinct laser nature.

Such SOA modules, whose small-scale production was started in 2005 (the SOA-371 model), can be used in single-frequency lasers with fibre Bragg gratings (FBGs) employed as external cavities. By using external cavities with controllable spectrally selective elements, it is possible to fabricate tunable lasers. As mentioned above, we used an AOTF as such an element in this paper.

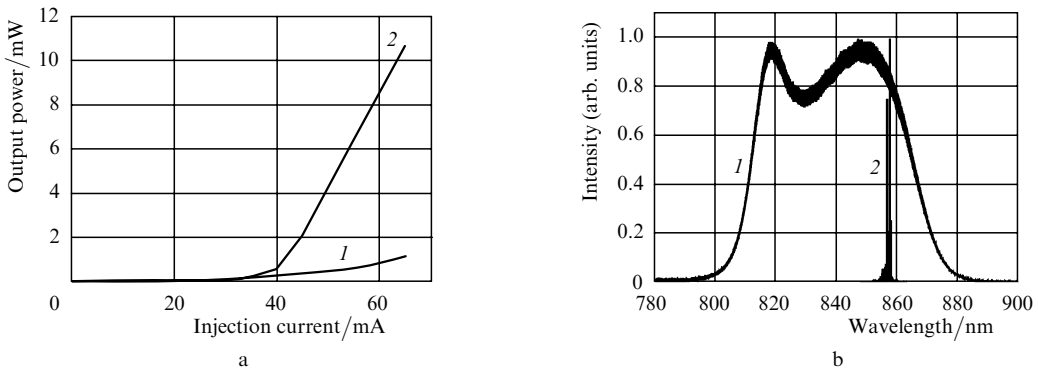

Figure 1. Light–current characteristics (a) and output emission spectra (b) of SOA modules in the SLD regime (*1*) (for the inclined cleave of the output SMF) and in the lasing regime (*2*) (for the perpendicular cleave).

The choice of the AOTF design was determined by the requirement of a high spectral resolution needed to obtain a sufficiently narrow laser line. In this connection the solution proposed in [6] seems to be the most promising. The principal difference of the geometry of this acousto-optic interaction from others used in AOTFs is that it does not provide the interaction of a diverging light beam with a sound wave because the tangents to the surfaces on which the ends of the wave vectors of the incident and diffracted light waves are not parallel to each other. The high resolution is achieved due to an increase in the length L of acousto-optic interaction. In the device under study, radiation with the nearly diffraction-limited divergence is used. Therefore, the abandonment of the requirement of wide-aperture interaction allowed us to realise such interaction between light and sound in a very efficient acousto-optic material – paratellurite (TeO_2).

The direction of the phase velocity was chosen close to that of the [110] crystallographic axis (the deviation was 2.2°). This provided high values of the acting coefficient of acousto-optic quality and birefringence Δn. The light beam was directed along the acoustic beam (Fig. 2). By calculating the FWHM of the AOTF instrumental function from the known expression $\Delta\lambda = \lambda^2/(\Delta nL)$ (where λ is the optical wavelength), we obtain for $\lambda = 840$ nm, $\Delta n = 0.145$ (TeO_2) and $L = 25$ nm the value $\Delta\lambda = 0.2$ nm, which is close to the spectral resolution directly measured for such AOTFs.

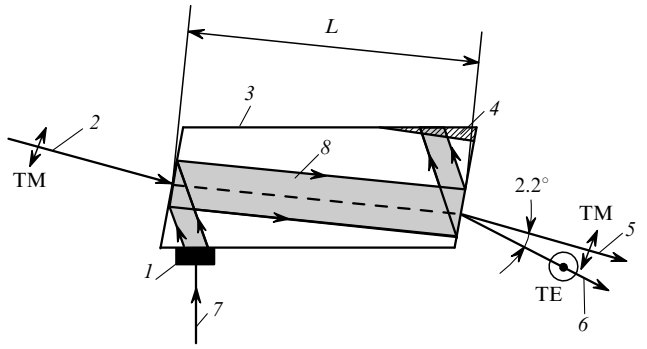

Figure 2. The AOTF scheme: (*1*) lithium niobate piezoelectric transducer; (*2*) incident polarised radiation; (*3*) paratellurite sound duct; (*4*) sound absorber; (*5*) transmitted light (zero diffraction order); (*6*) diffracted (filtered) radiation; (*7*) high-frequency signal at the AOTF input; (*8*) acoustic beam in a paratellurite crystal.

Based on the element described above and OZ Optics fibre collimators, we developed a monolithic AOTF with input and output Corning PANDA SMFs. The main characteristics of this device are presented below:

Spectral range/nm	750–950
Spectral resolution/nm	< 0.3
SMF/SMF coupling efficiency (%)	70
Switching time/μs	40
Polarisation	linear
SMF type	SM85-PS-025A

To provide a positive feedback and coupling radiation out of a fibre cavity, we developed the original design of a broadband semitransparent fibre mirror by using the modified manufacturing technology of broadband SMF couplers [7]. One of such couplers with the division coefficient 96 : 4 was used to couple a part of the output radiation to an automatic power control (APC) system.

Figure 3 shows the scheme of the laser. The electronic circuit of a commercial PILOT-4 SLD controller provided power supply for the SOA, its thermal stabilisation, and the constant output optical power in the APC regime. Only the cw injection regime for the SOA was used. The APC system could be switched off during experiments, and the SOA was

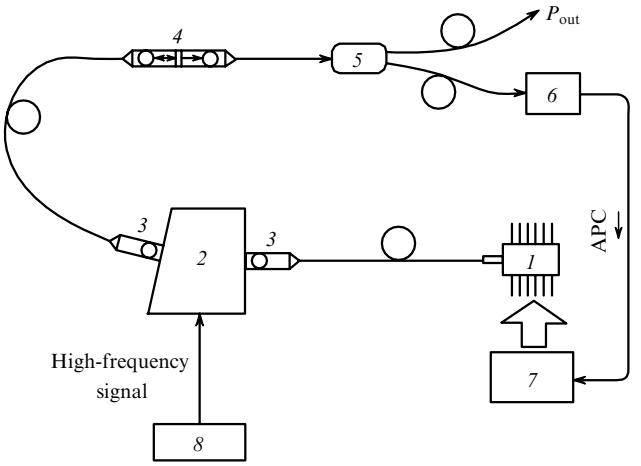

Figure 3. Scheme of a tunable semiconductor laser with an AOTF in an external fibre cavity: (*1*) SOA-371 module; (*2*) AOTF; (*3*) fibre collimator; (*4*) fibre mirror ($R = 30$ %); (*5*) fibre Y-coupler; (*6*) pin photodetector producing the input APC signal; (*7*) PILOT-4 SOA controller; (*8*) AOTF controller.

switched on to the automatic injection current control (ACC) regime. The block diagram of the original AOTF controller is shown in Fig. 4. This device provided the output high-frequency signal of power up to 1 W, which could be tuned in the frequency range from 85 to 113 MHz, which corresponds to the optical tuning range of the AOTF from 750 to 950 nm and overlaps with a great margin the SOA gain band. The frequency of the high-frequency signal (the central wavelength of the AOTF transmission spectrum) was determined by the control voltage V, which could be supplied from an external source or an in-built control voltage generator. The latter could supply a constant voltage or a saw-tooth voltage changing in time. The maximum rate of voltage variation (sweep frequency) noticeably exceeded the AOTF time response.

3. Output characteristics of the laser

Figure 5a shows the light – current characteristic in the SLD regime recorded in the zero diffraction order of the AOTF and the light – current characteristics recorded in the lasing regime for the AOTF tuned to a wavelength of 860 nm corresponding to the maximum optical gain. Compared to the curves in Fig. 1a, the lasing threshold was decreased and the corresponding decrease in the external quantum efficiency was observed. Figure 5b presents the emission spectra in the lasing and SLD regimes for the SOA injection current $I = 65$ mA. In the lasing regime, the AOTF was tuned to a wavelength of 840 nm corresponding to the central wavelength of superluminescence. In this case, the narrowing of the spectrum by more than three orders of magnitude was observed. The laser linewidth $\delta\lambda$ measured with an ADVANTEST-Q8347 analyser was $\sim$0.045 nm. In this band, a few hundreds of longitudinal modes of an external cavity of length 1.5 – 2 m were excited. The excess of the line maximum over the pedestal was more than 60 dB. The polarisation degree of the output radiation was 98.5 %.

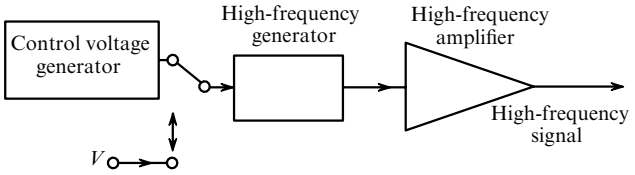

Figure 4. Block diagram of the AOTF controller.

Figure 6 shows the families of tuning curves of the laser in the ACC (without the output coupler) and APC regimes recorded upon a slow discrete variation of V.

As the SOA injection current increases, the tuning range of the laser in the ACC regime broadens due to the broadening of the SOA gain band [1, 2]. In the APC regime, the tuning range narrows down with increasing the level of the stabilised output power. The main factor limiting the output power P_{out} and the width of tuning range $\Delta\lambda_t$ is the requirement of a high reliability of the laser. In this case, the most critical element from the point of view of

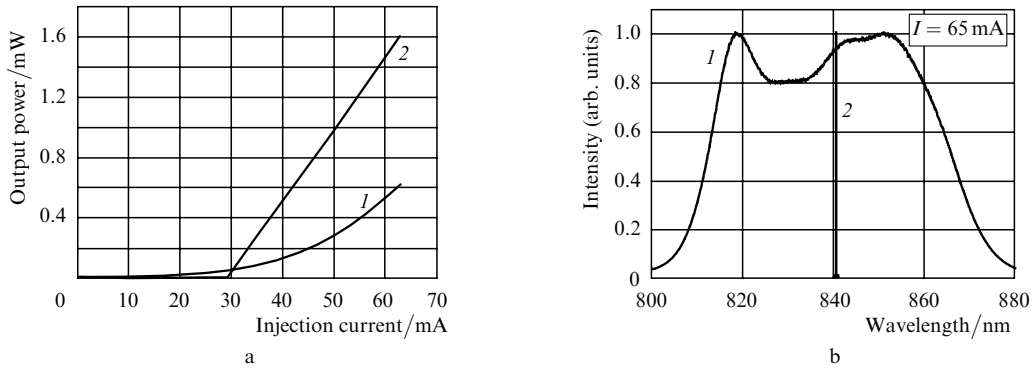

Figure 5. Light – current characteristics (a) and output emission spectra (b) of the SOA before placing it into a external cavity (*1*) and in the stationary laser regime (*2*) for the AOTF tuned to $\lambda = 860$ (a) and 840 nm (b).

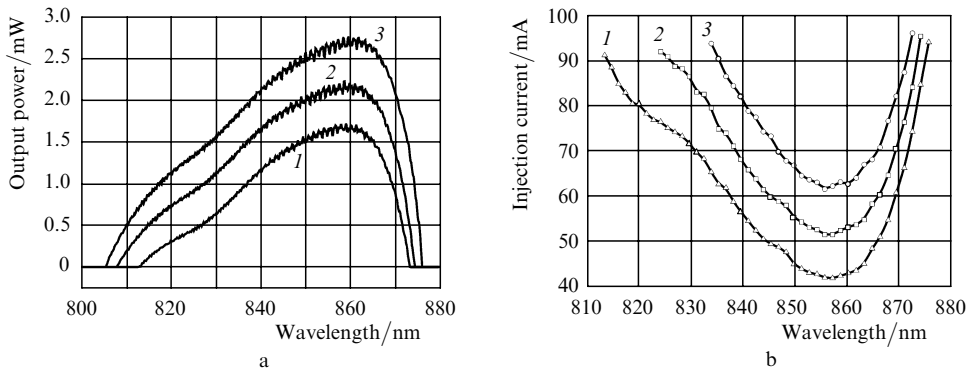

Figure 6. Tuning curves of the laser in the ACC regime for the SOA injection current equal to 65 (*1*), 75 (*2*), and 85 mA (*3*) (a) and in the APC regime for the output power equal to 0.5 (*1*), 1.0 (*2*), and 1.5 mW (*3*) (b).

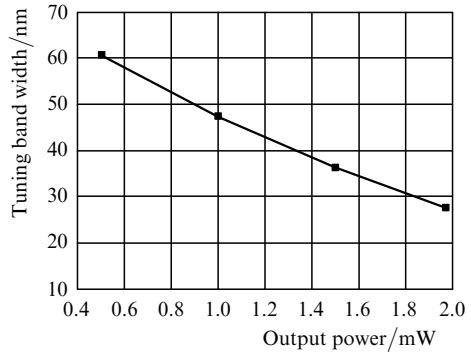

Figure 7. Width of the slow continuous tuning band of the laser as a function of its output power in the APC regime.

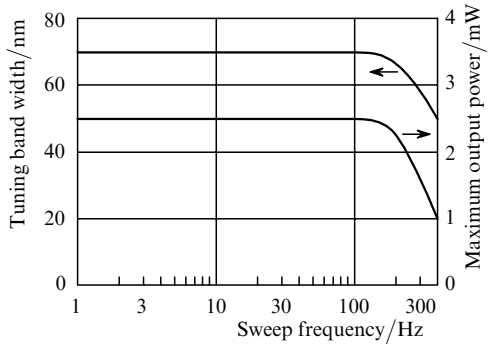

Figure 8. Maximum output power and the tuning band width of the laser in the ACC regime for $I = 85$ mA as functions of the sweep frequency for the amplitude ΔV corresponding to the AOTF tuning range from 800 to 880 nm.

the service life is the SOA. Our estimate shows that the output power $P_{out} = 2.0$ mW in the final scheme of the laser (Fig. 3) corresponds to the power $\sim$20 mW on the SOA output facet. Such a relation between the powers is determined by total optical losses at the coupling unit in the SOA module, fibre collimators, AOTF, Y-coupler, and SMF splices (not shown in Fig. 3).

Preliminary resource tests of SOA-371 modules showed that the service life of these devices decreased when the output power exceeded 20 mW. For this reason, the output power in the subsequent studies did not exceed this level and the SOA operating current was limited by 100 mA. In the APC regime, this value of the operating current determined the extreme points and the width $\Delta\lambda_t$ of the tuning band. The corresponding dependence is shown in Fig. 7.

Another factor limiting the output power and the width of the tuning range of the laser in the sweep regime is a finite time response of the AOTF. With increasing the sweep rate, which is determined by the rate of variation in the frequency of a high-frequency control signal, the chirp on a diffraction grating produced by an acoustic wave in the TeO_2 crystal increases, whereas the diffraction efficiency of the wave decreases. Figure 8 shows the dependences of the maximum output power for $\lambda = 860$ nm and the width of the tuning band on the sweep frequency for the constant amplitude of the control signal of the AOTF in the ACC regime for $I = 85$ mA. These dependences show that the output characteristics of the laser under study rapidly degrade upon sweeping within the entire tuning band at the frequency above 120 Hz. We decided finally in the course of laser modification to restrict the sweep frequency by 200 Hz. An increase in the fast response of the AOTF

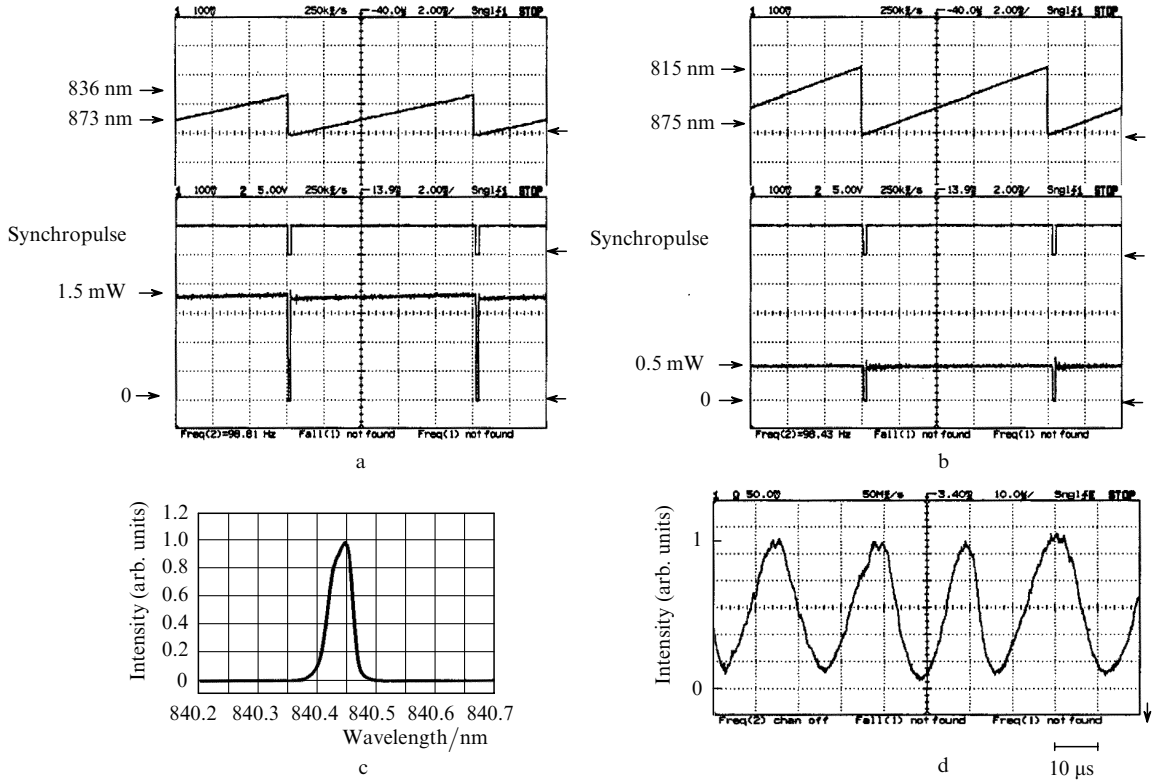

Figure 9. Oscillograms of the control voltage, synchrosignal, and output power in the APC regime for the sweep frequency 100 Hz, $P_{out} = 1.5$ (a) and 0.5 mW (b), and the stationary lasing spectrum (c) and the chronogram of radiation transmitted through the Fabry–Perot etalon (d) (sweep regime corresponding to Fig. 9a).

inevitably reduces its spectral resolution. To find the optimal parameters of the AOTF providing the maximum sweep frequency by preserving continuous spectral tuning, it is necessary to perform further studies.

Figure 9 shows the oscillograms of a control signal determining the laser wavelength, of synchropulses and the output laser power for the sweep frequency 100 Hz. The laser operated in the APC regime emitting 1.5 and 0.5-mW pulses (after the Y-coupler). For sweep frequencies up to 200 Hz, no increase in the 'instant' linewidth of the laser was observed compared to the case of stationary lasing. This is illustrated in Figs 9c, d. The first of them shows the stationary lasing spectrum, and the second one presents the chronogram of radiation transmitted through the Fabry–Perot etalon with the free spectral range of 0.09 nm in the sweep regime corresponding to Fig. 9a. The estimated 'instant' linewidth is $\sim$0.05 nm, which slightly differ from the stationary value.

4. Conclusions

Laser radiation sources with a rapid wavelength sweep attract recent interest of the researchers involved in the development of new systems of optical coherence tomography [8, 9]. Based on our studies, we have developed a laboratory prototype of a laser with the following technical parameters:

Spectral range/nm	815–875
Optical power at the SMF output/mW	
low-power regime	0.5
high-power regime	1.5
Tuning band width/nm	
low-power regime	60.0
high-power regime	37.0
Laser linewidth/nm	< 0.05
Side-mode suppression degree/dB	> 60
Sweep frequency/Hz	1–200

To our knowledge, such a laser emitting in the near-IR is developed for the first time.

Acknowledgements. The authors thank W. Dreksler for initiating this work and A.T. Semenov for his attention and support. This work was partially supported by the ISTC Grant No. 2651p.

References

1. Semenov A.T., Batovrin V.K., Garmash I.A., Shidlovski V.R., Shramenko M.V., Yakubovich S.D. *Electron. Lett.*, **31** (4), 314 (1995).
2. Batovrin V.K., Garmash I.A., Gelikonov V.M., Gelikonov G.V., Lyubarskii A.V., Safin S.A., Semenov A.T., Shidlovskii V.R., Shramenko M.V., Yakubovich S.D. *Kvantovaya Elektron.*, **23**, 113 (1996) [*Quantum Electron.*, **26**, 109 (1996)].
3. Coquin G.A., Cheung K.W. *Electron. Lett.*, **24** (10), 599 (1988).
4. Takabayashi K., Takada K., Nashimoto N., Doi M., Tomabechi S., Nakazava T., Morito K. *Electron. Lett.*, **40** (19), 1187 (2004).
5. Semenov A.T., Shidlovski V.R., Safin S.A. *Electron. Lett.*, **29** (10), 854 (1993).
6. Voloshinov V. *Opt. Eng.*, **31** (10), 2089 (1992).
7. Adler D.S., Ko T.H., Konorev A.K., Mamedov D.S., Prokhrov V.V., Fujimoto J.J., Yakubovich S.D. *Kvantovaya Elektron.*, **34**, 915 (2004) [*Quantum Electron.*, **34**, 915 (2004)].
8. Nielsen F.D., Thrane L., Black J., Hsu K., Bjarklev A., Andersen P.E. *Proc. SPIE-OSA Biomed Opt.*, **5861**, 58610H-2 (2005).
9. Huber K., Taira K., Wojtkowski M., Fujimoto J.G. *Proc. SPIE-OSA Biomed Opt.*, **5861**, 586111B-1 (2005).